Physics AUC, vol. 34, 117-127 (2024) PHYSICS AUC

Contribution to the Study of Riblet Sizing on Multiform Bodies in Incompressible Subsonic Flow

Faris Aissaoui[*,1,2], Yousef Belloufi[1,3], Amar Rouag[4,5], Abdelhafid Brima[1], Abdelmoumene Hakim Benmachiche[6], Khalid Faiza[7], Faouzi Akermi[2]

[1] Laboratoire de Génie Mécanique, LGM, Université de Biskra, B.P.145 R.P. 07000 Biskra, Alegria.
[2] Université De Ghardaia, Faculté Des Sciences Et De La Technologie, Département D'automatique Et Electromécanique, Ghardia47000, Algeria.
[3]Univerité Kadi Merbah Ouargla, Faculté Des Hydrocarbures, Des Energies Renouvelables, Des Science De La Terre Et De L'univers, Département De Forage Et Mécanique Des Chantiers Pétroliers BP 511 Ouargla 30000, Algeria.
[4]Univerité Kadi Merbah Ouargla, Faculté Des Hydrocarbures, Des Energies Renouvelables, Des Science De La Terre Et De L'Univers, Département Des Energies Renouvelables, BP 511 Ouargla 30000, Algeria.
[5] Laboratoire De Génie Energétique Et Matériaux (LGEM), Université Mohamed Khider Biskra, B.P.145 R.P. 07000 Biskra, Alegria.
[6] Département de Physique, Université de Batna, Algria.
[7] Département de Mécanique, Université de Batna, Algria.

* Corresponding author, Email address: techno_fares@yahoo.fr

Abstract

Our research focuses on contributing to the sizing study of riblets on multiform bodies in incompressible subsonic flow. We tackled this issue experimentally using a subsonic wind tunnel. The experiment involved measuring the drag on three smooth-walled bodies (sphere, ogive, wing) at various flow velocities. By analyzing the experimental data, we were able to determine the optimal riblet dimensions to apply on the surfaces of the tested bodies. The primary goal was to assess the riblets' effectiveness in reducing drag. Our findings indicate a potential for significant drag reduction, which can improve the aerodynamic performance of these bodies in subsonic flow conditions.

Keywords: Subsonic flow, wing, drag, sizing, riblets.

1. Introduction

Renewable energy sources, such as solar, wind, and hydroelectric power, are becoming increasingly important in the quest for sustainable development and environmental conservation**.[1-3]** Aerodynamics is one of the branches of fluid mechanics. It is specifically devoted to the study of air flow and, more practically, around obstacles. Examples of applications of aerodynamics include studying an airplane's movement in flight, analyzing wind forces on a building, and understanding the operation of a windmill. The development of aerodynamics has paralleled advancements in other sciences, such as computing, with increasingly powerful computers despite their cost, experimental techniques (wind tunnel testing), and of course, mathematics, with significant progress in numerical techniques for solving the generalized NAVIER-STOKES equations in fluid mechanics.

For several years, researchers in fluid mechanics and energy have made significant efforts to reduce friction drag, knowing that it represents about 40 to 50% of the total drag of a transonic transport aircraft. Among the passive methods generally studied, we find the control of shock wave/boundary layer interaction by implementing porous surfaces and cavities with different geometric characteristics and modifying the wall geometry using longitudinal grooves or "riblets." This second technique seems the most attractive because it is relatively easy to implement and very promising for aircraft application. In the following, we will present the important works and results conducted in various laboratories worldwide. For controlling shock wave/boundary layer interaction. Bur et al.[4] mentioned that this control technique was suggested by Bushnell Whicomb from the NASA Langley Research Center in 1979. From 1980 onwards, these works were continued by Nagmatsu from the Rensselaer Polytechnic Institute. Thus, Bahi et al. [5] applied passive control to a supercritical profile mounted on the wall of a small transonic channel. A study conducted by Ider et al. [6]at CERT-ONERA, as part of transonic profile drag reduction, also implemented the passive control technique. Despite purely experimental difficulties, it seemed that significant gains were envisaged by reducing the hole diameter to the order of a tenth of a millimeter to ensure better distribution of transverse flows and having low roughness. Riblet structures usually have heights ranging from a few micrometers to several hundred micrometers. Their function is to inhibit the lateral movement of coherent turbulent structures near the wall (e.g., [7]).

In addition to experimental efforts, several numerical simulations have provided a deep understanding of turbulent flow and the behavior of coherent vertical structures near riblets (e.g., [8-11]). Recently, Garcia-Mayoral and Jimenez [12], using direct numerical simulations, proposed a new parameter for evaluating riblet performance: the non-dimensional square root of the groove cross-section. This parameter appears to better unify the different results obtained by various researchers.Some experimental studies have focused on the performance of riblets on airfoils. Experiments using a NACA 0012 airfoil section at relatively low Reynolds numbers [13-15]have shown drag reduction. Although this airfoil section is not used in wind turbines, its well-documented performance makes it an excellent subject for comparative analysis with riblets.

In this context, our work aims to contribute to the study of riblet sizing on multiform bodies in incompressible subsonic flow. This work is based on an experimental study of the drag of these bodies conducted in a subsonic wind tunnel. The primary objective is to determine the optimal dimensions and configurations of riblets that can be applied to the surfaces of different bodies to minimize drag. We conducted experiments on three different smooth-walled bodies: a sphere, an ogive, and a wing. For each of these bodies, we measured drag at various flow velocities. The experimental setup included a subsonic wind tunnel equipped with precise measurement instruments to capture data on the aerodynamic forces acting on the bodies. By analyzing this data, we aimed to understand how riblets affect the flow dynamics and drag characteristics of each body type.

Our analysis involved comparing the drag measurements of smooth-walled bodies with those modified with riblets. We examined how different riblet geometries influenced the drag reduction and identified the most effective configurations. This research has the potential to significantly enhance the aerodynamic performance of various structures, particularly in aviation, by reducing friction drag and improving overall efficiency. Our study provides

valuable insights into the design and application of riblets for drag reduction in incompressible subsonic flow. The experimental results highlight the importance of precise riblet sizing and configuration for maximizing their effectiveness. This research contributes to the broader field of aerodynamics and fluid mechanics, offering practical solutions for improving the performance of multiform bodies in subsonic flow conditions.

2. Experimental set-up

The machine utilized was specifically designed for testing and demonstrations in aerodynamics and fluid dynamics (see figure 1). It is an open-circuit subsonic wind tunnel with a square test section. With a wide range of available accessories, it enables a variety of tests to be performed, including:

Comparing different methods for measuring velocity and pressure.

Determining the drag coefficient of various bodies (disk, cone, aerodynamic bodies, half-wing)(see figure 2.).

Measuring the resistance and thrust coefficients of half-wings at different angles of incidence.

Studying boundary layers.

Sphere Ogive wing

Figure 1. different solid bodies used.

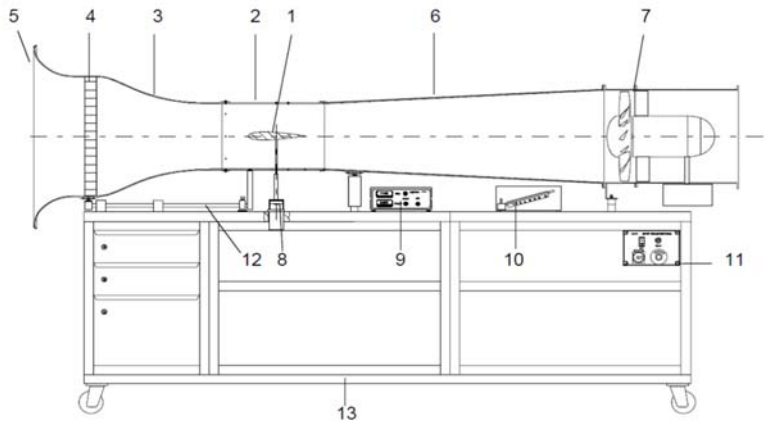

Figure 2. Operation of the wind tunnel

1. Model.
2. Measurement section.
3. Nozzle.
4. Flow stabilizer.
5. Inlet cone.

6. Diffuser.
7. Axial fan.
8. Two-component electronic force transducer.
9. Measurement amplifier with force display.
10. Inclined tube manometer for airspeed.
11. Control box with fan speed adjustment.
12. Guide for translatable nozzle.
13. Laboratory cart with drawers.

3. Drag measurement

We conducted measurements on the bodies shown in Figure 1. Table 1 presents the key characteristics of our work measured on the wing.

Table 1. Aerodynamic characteristics of the wing.

Velocity V (m/s)	Drag T (N)	Pressure (m bars)	Mach number M	Drag coefficient C_x	Reynolds number Re
4	0	0,1	0,01174571	0	26490,0662
5	0	0,175	0,01468213	0	33112,5828
6	0	0,225	0,01761856	0	39735,0993
7	0	0,325	0,02055498	0	46357,6159
8	0,01	0,425	0,02349141	0,03125	52980,1325
9	0,01	0,525	0,02642784	0,02469136	59602,649
10	0,01	0,65	0,02936426	0,02	66225,1656
11	0,02	0,775	0,03230069	0,03305785	72847,6821
12	0,02	0,9	0,03523712	0,02777778	79470,1987
13	0,02	1,05	0,03817354	0,02366864	86092,7152
14	0,02	1,2	0,04110997	0,02040816	92715,2318
15	0,02	1,4	0,0440464	0,01777778	99337,7483
16	0,03	1,6	0,04698282	0,0234375	105960,265
17	0,03	1,8	0,04991925	0,02076125	112582,781
18	0,04	2	0,05285567	0,02469136	119205,298
19	0,04	2,25	0,0557921	0,02216066	125827,815
20	0,05	2,45	0,05872853	0,025	132450,331
21	0,06	2,75	0,06166495	0,02721088	139072,848
22	0,07	2,95	0,06460138	0,02892562	145695,364
23	0,09	3,225	0,06753781	0,03402647	152317,881
24	0,1	3,55	0,07047423	0,03472222	158940,397
25	0,11	3,85	0,07341066	0,0352	165562,914
26	0,12	4,15	0,07634709	0,03550296	172185,43
27	0,13	4,455	0,07928351	0,03566529	178807,947
28	0,15	4,8	0,08221994	0,03826531	185430,464
29	0,16	5,15	0,08515636	0,03804994	192052,98

4. Designing "RIBLETS"

It is important to note that a 20% reduction in aerodynamic drag of airplanes, trains, and automobiles results in a 10% reduction in energy consumption (this is an interesting percentage).
Controlling turbulence increasingly involves manipulating coherent vortices to either intensify them (in combustion and chemical engineering) or reduce them (in hydrodynamics, aerodynamics, acoustics, and hydro-elasticity).
In the absence of being able to eliminate vortices, efforts can be made to alter their shape and organization... Turbulence control remains an emerging and largely empirical science, but the rapid development of numerical simulations is certainly expected to advance it significantly.
In aerodynamics, boundary layer suction delays boundary layer separation. To reduce drag, extensive research has also been conducted on self-adapting surfaces and polymer injections into the wall, which reduce turbulence. Indeed, the most effective method for reducing drag in aerodynamics and hydrodynamics appears to be "riblets."
Riblets refer to flow-aligned grooved surfaces originally developed at NASA Langley Research Center in the early 1970s to reduce turbulent friction. They can also be defined as fine longitudinal ridges placed along the flow direction on the surface, resembling corduroy fabric (see Figure 4). Riblets are characterized by three essential geometric parameters:
Base (b)
Spacing (s)
Height (h)
The parameter L represents the manipulated boundary layer length.

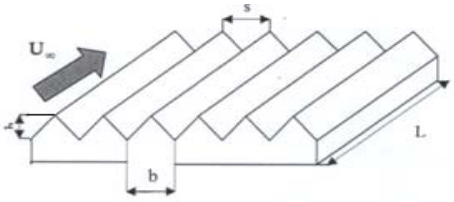

Figure 3. Diagram of "riblets" [16]

The viscous drag D is given by the integral below:

$$D = \int \tau_w dS \quad (1)$$

When the frictional force is uniform, therefore::

$$D = \tau_w . S \quad (2)$$

With
D : drag; S : surface ; τ_w : Friction stress
The friction speed is given by the expression below:

$$U_\tau = \sqrt{\frac{\tau_w}{\rho}} \quad (3)$$

As per [17], the optimal passive control ensuring friction reduction occurs for the dimensionless parameters $S^+$and h^+ close to 13. It is noted that a maximum of 8% reduction in friction drag compared to a smooth surface is achieved for these $S^+$and h^+.values. To

design riblets, it is necessary to consider the values of friction velocities found in the study of flow over a smooth wall, such as:

$$S^+ = \frac{SU_\tau}{\upsilon} \quad \text{et} \quad h^+ = \frac{hU_\tau}{\upsilon} \tag{4}$$

So, for the worst-case scenario corresponding to the maximum friction velocity value over the smooth surface case, we calculate the two geometric parameters S and h. For the maximum stress value U (see table 2).We calculate the crest dimensionsS.

$$\frac{SU_\tau}{\upsilon} \leq 13 \tag{5}$$

$$S \leq \frac{13\upsilon}{U_\tau} \tag{6}$$

We have

$$U_{\tau max}=3{,}63636364 \text{ (m/s)}$$

We take the value of S such that

$S \leq 0.053625$mm. What we call micro-grooves

Table 2. Calculations of frictional stress and friction velocity for the wing case.

Velocity V (m/s)	Drag T (N)	Friction stress τ_w(N/m^2)	Velocity of friction U(m/s)
4	0	0	0
5	0	0	0
6	0	0	0
7	0	0	0
8	0,01	1	0,90909091
9	0,01	1	0,90909091
10	0,01	1	0,90909091
11	0,02	2	1,28564869
12	0,02	2	1,28564869
13	0,02	2	1,28564869
14	0,02	2	1,28564869
15	0,02	2	1,28564869
16	0,03	3	1,57264329
17	0,03	3	1,57459164
18	0,04	4	1,81818182
19	0,04	4	1,81818182
20	0,05	5	2,03278907
21	0,06	6	2,22680886
22	0,07	7	2,40522846
23	0,09	9	2,72727273
24	0,1	10	2,87479787
25	0,11	11	3,01511345
26	0,12	12	3,14918329
27	0,13	13	3,27777389
28	0,15	15	3,52089395
29	0,16	16	3,63636364

5. Results and discussions

Figure 4 illustrates the variation of drag as a function of flow speed. We notice that: as the speed increases, the drag increases. For comparison, we notice that: the drag of the wing is less than that of the ogive and the sphere due to the geometric shape. Therefore, it is preferable to choose suitable aerodynamic shapes.

"Figures 5,6 and 7 represent the variation of the drag coefficient Cx as a function of the Reynolds number Re. As the Reynolds number increases, the drag coefficient increases. We also notice:

If the Reynolds number reaches the value 10^5, where the air flow is in a transitional regime, the drag coefficient remains constant at a value close to 0.5 for the sphere and at 0.04 for the ogive.

On the other hand, the drag coefficient of the wing increases up to the value of 0.035, stabilizing at this value when the Reynolds number is greater than or equal to 1.6×10^5."

To clearly see the influence of the angle of inclination on the value of drag for different flow speed values, the corresponding variation laws are represented in Figure 8.

Figure 8 provides a detailed visualization of how the drag changes with different angles of inclination relative to the horizontal plane for the wing. By examining these variation laws, one can better understand the aerodynamic behavior under varying conditions and make informed decisions about the optimal angles to minimize drag. This understanding is crucial for designing efficient aerodynamic shapes and improving overall performance in various applications.

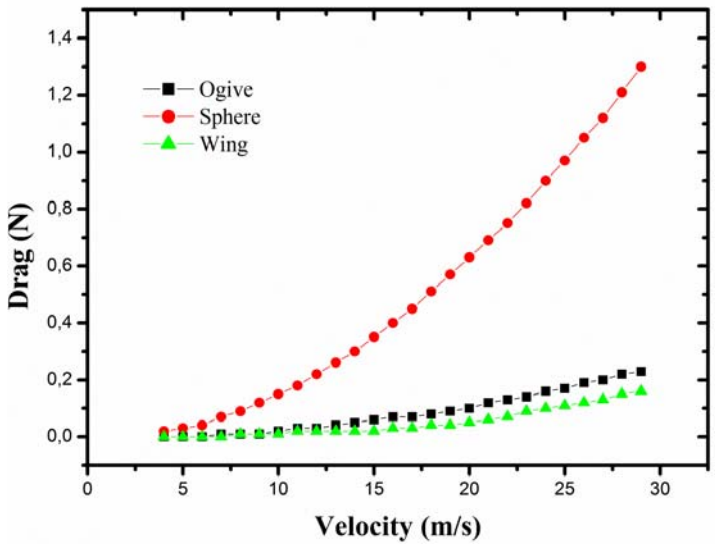

Figure 4. Variations in drag as a function of speed for different solid bodies

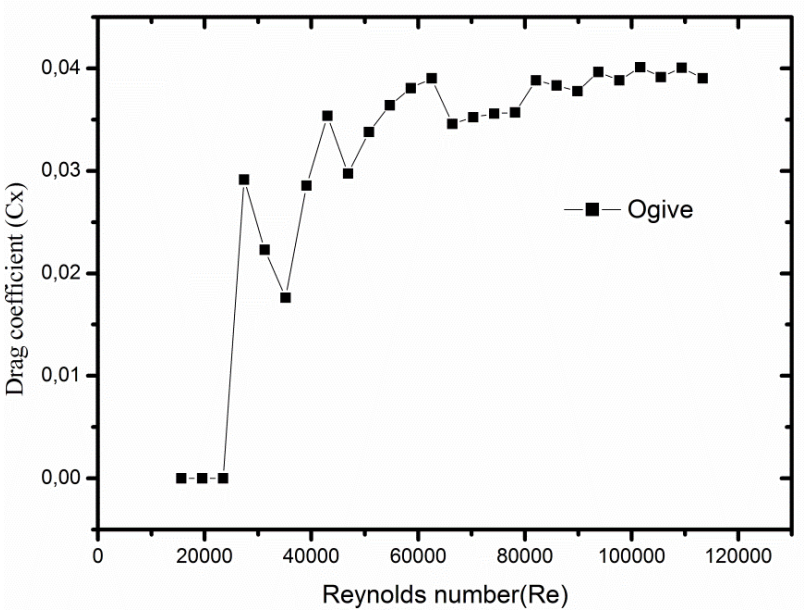

Figure 5. Variation of drag coefficient Cx as a function of Reynolds number (case of the ogive)

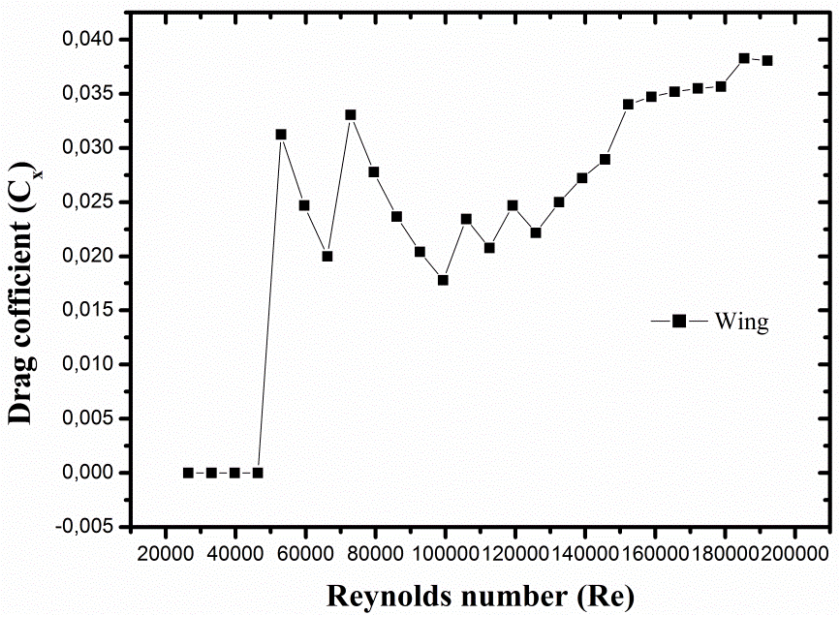

Figure 6. Variation of drag coefficient Cx as a function of Reynolds number Re (case of the wing

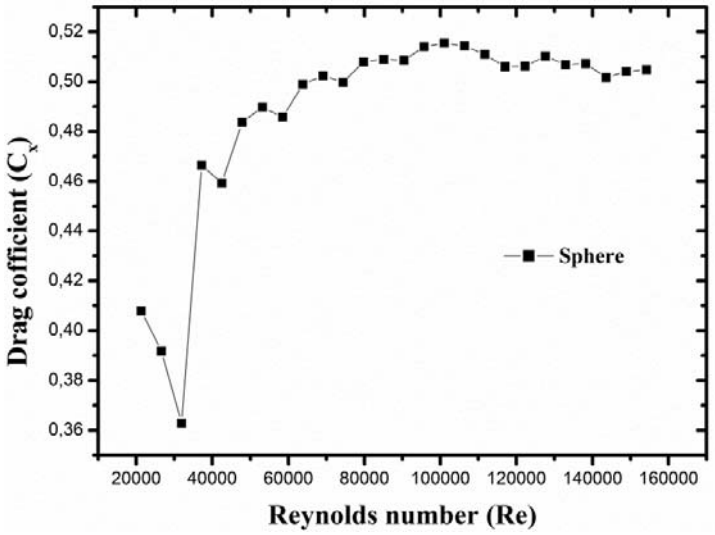

Figure 7. Variation of drag coefficient Cx as a function of Reynolds number (case of the sphere)

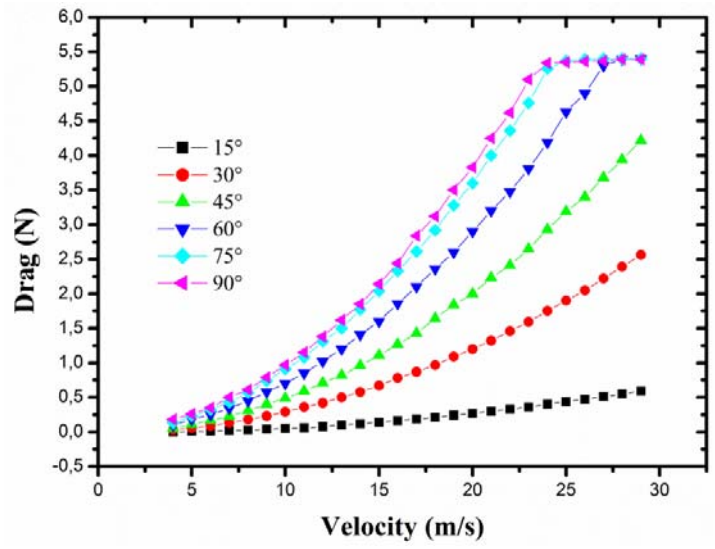

Figure 8. Variation of drag as a function of speed for different angles of inclination relative to the horizontal of the wing.

6. Conclusion

The initial focus of this study was on calculating drag based on measurements taken from three smooth bodies (sphere, ogive, wing). Riblets were designed using the calculated maximum friction velocities. Continuing this investigation, we explored the influence of two parameters, Reynolds number and inclination angle, on drag: drag increases with higher inclination angles and Reynolds numbers.

Finally, based on our findings, it is clear that grooves significantly reduce drag. This observation underscores the effective drag reduction capabilities of grooves, suggesting their potential for practical applications in minimizing aerodynamic resistance and enhancing overall efficiency in fluid dynamics.

Nomenclature

U, V	Velocity component	m/s
S	Surface	m^2
$\boldsymbol{U_\infty}$	Axial velocity at infinity	m/s
$\boldsymbol{\vec{q}}$	Velocity vector	m/s
p	Pressure	Kg/ms^2
(x,y)	Cartesian coordinates	m
$\boldsymbol{D}$	Drag	N
$\boldsymbol{\vec{n}}$	Unit normal vector to a surface element	
$\mathbf{U}_{\boldsymbol{\tau}}$	Average friction velocity	m/s
$\boldsymbol{\tau_w}$	Friction stress	N/ m^2

Greek characters

λ	Thermal conductivity	w/m k° s
μ	Dynamic viscosity	Kg/ m s
ν	Kinematic viscosity	m^2/s

Dimensionless numbers

$\mathbf{C_x}$	Drag coefficient	$\boldsymbol{F_x}/\mathbf{2}\ \rho SV^2$
Re	Reynolds number	VD/ς
M	Mach number	V/ς

References

[1] F. Aissaoui, Contribution à l'étude de transfert de chaleur d'un capteur solaire placé dans un climat aride: cas de la région de Biskra, Université Mohamed Khider-Biskra, 2017.

[2] F. Aissaoui, A. H. Benmachiche, A. Brima, D. Bahloul and Y. Belloufi, Experimental and theoretical analysis on thermal performance of the flat plate solar air collector, *International Journal of Heat and Technology*, vol. 34 2, pp. 213-220, 2016.

[3] F. Aissaoui, A. H. Benmachiche, A. Brima, Y. Belloufi and M. Belkhiri, Numerical study on thermal performance of a solar air collector with fins and baffles attached over the absorber plate Numerical study on thermal performance of a solar air collector with fins and baffles attached over the absorber plate, vol. pp.

[4] R. Bur, Etude fondamentale sur le controle passif de l'interaction onde de choc/couche limite turbulente en ecoulement transsonique, Paris 6, 1991.

[5] L. Bahi, J. Ross and H. Nagamatsu, Passive shock wave/boundary layer control for transonic airfoil dragreduction, Presented at 21st Aerospace Sciences Meeting, pp. 137, 1983.

[6] H. Ider and M. Illoul, Contrôle actif par soufflage du décollement naissant à l'extrados du profil NACA 0015, Université Mouloud Mammeri Tizi-Ouzou, 2017.

[7] K.-S. Choi, Near-wall structure of a turbulent boundary layer with riblets, *Journal of fluid mechanics,* vol. 208 pp. 417-458, 1989.

[8] P. S. Bernard, J. M. Thomas and R. A. Handler, Vortex dynamics and the production of Reynolds stress, *Journal of fluid mechanics,* vol. 253 pp. 385-419, 1993.

[9] H. Choi, P. Moin and J. Kim, Direct numerical simulation of turbulent flow over riblets, *Journal of fluid mechanics,* vol. 255 pp. 503-539, 1993.

[10] D. C. Chu and G. E. Karniadakis, A direct numerical simulation of laminar and turbulent flow over riblet-mounted surfaces, *Journal of fluid mechanics,* vol. 250 pp. 1-42, 1993.

[11] A. G. Kravchenko, H. Choi and P. Moin, On the relation of near-wall streamwise vortices to wall skin friction in turbulent boundary layers, *Physics of Fluids A: Fluid Dynamics,* vol. 5 12, pp. 3307-3309, 1993.

[12] R. Garcia-Mayoral and J. Jiménez, Hydrodynamic stability and breakdown of the viscous regime over riblets, *Journal of fluid mechanics,* vol. 678 pp. 317-347, 2011.

[13] J. Caram and A. Ahmed, Development of the wake of an airfoil with riblets, *AIAA journal,* vol. 30 12, pp. 2817-2818, 1992.

[14] M. Han, H. C. Lim, Y.-G. Jang, S. S. Lee and S.-J. Lee, Fabrication of a micro-riblet film and drag reduction effects on curved objects, Presented at TRANSDUCERS'03. 12th International Conference on Solid-State Sensors, Actuators and Microsystems. Digest of Technical Papers (Cat. No. 03TH8664), pp. 396-399, 2003.

[15] S. Sundaram, P. Viswanath and S. Rudrakumar, Viscous drag reduction using riblets on NACA 0012 airfoil to moderate incidence, *AIAA journal,* vol. 34 4, pp. 676-682, 1996.

[16] E. Coustols, Effet des parois rainurées («riblets») sur la structure d'une couche limite turbulente, *Mécanique & industries,* vol. 2 5, pp. 421-434, 2001.

[17] M. Walsh, Turbulent boundary layer drag reduction using riblets, Presented at 20th aerospace sciences meeting, pp. 169, 1982.